

# Spaceborne Doppler Precipitation Radar: system configurations and performance analysis

Simone Tanelli and Eastwood Im  
Jet Propulsion Laboratory, California Institute of Technology, Pasadena CA, USA

## ABSTRACT

Knowledge of the global distribution of the vertical velocity of precipitation is important in the study of energy transportation in the atmosphere, the climate and weather. Such knowledge can only be directly acquired with the use of spaceborne Doppler precipitation radars. Although the high relative speed of the radar with respect to the rainfall particles introduces significant broadening in the Doppler spectrum, recent studies have shown that the average vertical velocity can be measured to acceptable accuracy levels by appropriate selection of radar parameters. Furthermore, methods to correct for specific errors arising from NUBF effects and pointing uncertainties have recently been developed. In this paper we will present the results of the trade studies on the performances of a spaceborne Doppler radar with different system parameters configurations. Particular emphases will be placed on the choices of: 1) the PRF vs. antenna size ratio, 2) the observational strategy, 3) the operating frequency; and 4) processing strategy. The results show that accuracies of 1 m/s or better can be achieved with the currently available technology.

Keywords: Precipitation, Airborne Doppler Radar

## 1. DOPPLER VELOCITY MEASUREMENTS FROM SPACEBORNE RADAR

Doppler velocity measurements require coherent processing of the radar signal. It follows that two consecutive radar echoes must be correlated in order to allow the measurement of the relative phase shift (and therefore of the Doppler frequency shift) without ambiguity.

A Doppler radar transmitting one pulse every  $T_S$  seconds can measure without ambiguity the Doppler velocity of a single target in the range  $\pm v_m$  where  $v_m$  is the Nyquist limit imposed by the finite sampling:

$$v_m = PRF \cdot \lambda / 4. \quad (1)$$

where  $\lambda$  is the radar operating wavelength and  $PRF = 1/T_S$  is the Pulse Repetition Frequency. A Precipitation Radar measures the echo returned by the distributed target consisting of all hydrometeors within a radar volume of resolution, therefore, in general, the Doppler signal is described through its Doppler velocity spectrum  $P(v)$  which can be expressed as:

$$P(\mathbf{p}_s, \mathbf{r}_v, v) = \iiint \eta_R[\mathbf{p}_s + \mathbf{r}, v - v'] W(\mathbf{r}, \mathbf{r}_v) d\mathbf{r} \quad (2)$$

where  $\mathbf{p}_s$  is the satellite vector position,  $\mathbf{r}$  is the vector position relative to the satellite,  $W(\mathbf{r}, \mathbf{r}_v)$  is the radar weighting function for a given resolution volume centered at  $\mathbf{r}_v$ ,  $\eta_R(\mathbf{p}, v)$  is the reflectivity of a precipitation target at position  $\mathbf{p}$  and velocity  $v$  relative to  $\mathbf{p}_s$  [in this paper we adopt the convention of negative Doppler velocities for targets approaching the radar, so that  $v = -\lambda f/2$  where  $f$  is the Doppler frequency], and  $v'$  is the Doppler velocity shift due to satellite motion which can be written for NDPR as<sup>1</sup>:

$$v' = -q_{xv} (\mathbf{r} \cdot \mathbf{i}_x) \quad (3)$$

where  $\mathbf{i}_x$  is the versor corresponding to the flight direction and  $q_{xv}$  is the Doppler shift rate due to the motion of the satellite

$$q_{xv} = v_s / (\mathbf{r} \cdot \mathbf{i}_z) \cong v_s / h_s \quad (4)$$

where  $\mathbf{i}_z$  is the versor corresponding to the satellite's nadir and  $h_s$  is the spacecraft altitude.

The radar volume of resolution is defined by the radar weighting function  $W(\mathbf{r}, \mathbf{r}_V)$  which can be separated into two components by using a spherical coordinate system to represent  $\mathbf{r}$ :

$$W(\mathbf{r}; \mathbf{r}_V) = \frac{C \cdot G_a^2(\theta, \phi) \cdot |G_r(r - r_V)|^2}{L(r) \cdot r^4} \quad (5)$$

where  $C$  is the radar constant,  $G_a$  is the antenna gain pattern,  $G_r$  is the range weighting function, and  $L$  is the two-way atmospheric attenuation. In general, the volume of resolution of a Precipitation Radar is large enough to allow one to adopt a statistical representation of the distribution of scatterers inside it, the discrete distribution  $\eta_R(\mathbf{p}, v)$  can be therefore represented by a continuous probability function.

$$\eta_R[\mathbf{p}, v] = \sigma_b [D(\mathbf{p}, v)] N [D(\mathbf{p}, v)] \frac{dD(\mathbf{p}, v)}{dv} \otimes T(\mathbf{p}, v) \quad (6)$$

where  $\sigma_b$  and  $N$  are the particle backscattering cross-section and the specific number concentration for a generic hydrometeor kind, respectively, and  $D(\mathbf{p}, v)$  is the hydrometeor diameter expressed as function of its vertical velocity, that is,  $D(\mathbf{p}, v)$  is the inverse function of

$$v(\mathbf{p}, D) = [u_x(\mathbf{p}) + v_t(\mathbf{p}, D)](\mathbf{r} \cdot \mathbf{j}_z) + u_x(\mathbf{p})(\mathbf{r} \cdot \mathbf{j}_x) + u_y(\mathbf{p})(\mathbf{r} \cdot \mathbf{j}_y) \quad (7)$$

where  $u(\mathbf{p})$  is the background wind in the three directions  $\mathbf{j}_x, \mathbf{j}_y$  [horizontal] and  $\mathbf{j}_z$  [vertical, positive downward].  $v_t(\mathbf{p}, D)$  is the terminal velocity vs. particle diameter relation, the dependency on position is included only to account for the dependence of the terminal velocity on the air density, and therefore altitude. The small-scale turbulence of the air is accounted for through the Gaussian spread function  $T$ .

## 2. DOPPLER SPECTRUM WIDTH

A first assessment of the characteristics of the Doppler velocity spectrum described by (2) is generally obtained by assuming a uniformly filled volume of resolution<sup>2,3</sup>. In other words, it is assumed that  $N(\mathbf{p}, D) = N(D)$  within the volume of resolution. Any one of the commonly adopted analytical forms for  $N(D)$  and  $v_t(D)$  can be considered here - see Meneghini and Kozu<sup>4</sup> for examples. The three wind components are assumed to vary with constant wind shear factors within the volume of resolution. Also, the antenna pattern within the mainlobe is approximated with a Gaussian. Under these assumptions, the Doppler spectrum is approximated by a Gaussian and four independent, contributions to the Doppler spectrum width  $w$  are examined:

$$w^2 = w_D^2 + w_T^2 + w_K^2 + w_S^2 \quad (8)$$

- 1)  $w_D$  is the velocity spread due to different terminal velocities. It is determined by  $N(D)$ ,  $v_t(D)$  and, to a lesser extent, by  $\sigma_b(D)$  which, in turn, depends on the choice of radar operating wavelength. Its value is typically around  $1 \text{ m s}^{-1}$ . The Doppler spectrum associated with the terminal fall velocities is often approximated with a Gaussian, although it is actually slightly skewed, and its mean velocity is typically in the 1 to 7 m/s range.
- 2)  $w_T$  is the velocity spread due to turbulence. Values for  $w_T$  of 1 and 4 m/s are associated with standard and extreme turbulence, respectively. Such broadening is well approximated by a zero-mean Gaussian spectrum.
- 3)  $w_K$  is the broadening due to wind shear. Its contribution has been widely studied and a comprehensive discussion of the effect of wind shear for an NDPR with circularly symmetric antenna pattern can be found in 5, whence the following expression is obtained:

$$w_K^2 = \frac{\theta_{3dB}^2 h_S^2}{4a} (w_{Kzx}^2 + w_{Kzy}^2 + w_{Kh}^2) + w_{Kzz}^2 \quad (9)$$

where

$$\begin{aligned} w_{Kzx}^2 &= (u_{x0} / h_S + K_{zx})^2 \\ w_{Kzy}^2 &= (u_{y0} / h_S + K_{zy})^2 \\ w_{Kh}^2 &= \frac{\theta_3^2}{4a} (K_{xy} + K_{yx})^2 \\ w_{Kzz}^2 &= \left( \frac{0.35 K_{zz} c \tau_{pulse}}{2} \right)^2 \end{aligned} \quad (10)$$

where  $u_i = u_{i0} + jK_{ij}$  (the subscripts  $i=x, y, z$  and  $j=x, y, z$  indicate the direction of the wind component and the wind

shear component direction, respectively),  $c$  is the speed of light and  $\tau_{pulse}$  is the radar pulse duration. The parameter  $a$  depends on the approximation used for the antenna pattern (e.g.,  $a=2.6$  for the aperture type approximation used in<sup>5</sup>, while  $a=4\ln(2)\cong 2.77$  for a Gaussian approximation as in<sup>3</sup>). Note that (9) includes also the broadening effect of the average wind components across the beam (i.e.,  $u_{x0}$  and  $u_{y0}$ ), this is due to the fact that the associated radial velocity varies with the angle respect to the radar pointing direction. In general, it is found that  $K$  ranges between  $0.001\text{ s}^{-1}$  to  $0.01\text{ s}^{-1}$ .

- 4)  $w_S$  is the broadening due to the platform motion. Its effect can be immediately understood through the formalism used for calculating the wind shear by noting that the apparent average wind velocity should be used in (10) (i.e.,  $u_{x0}$  should be replaced by  $u_{x0} - v_s$ ) and therefore:

$$w_S^2 = \frac{\theta_{3dB}^2}{4a} v_S^2 \quad (11)$$

In general, all these causes of broadening must be accounted for. However, the following considerations help to simplify the problem:

- 1) Given a  $v_s$  of 7 km/s or higher, typical for a LEO satellite, the term  $w_S$  prevails over  $w_{Kxz}$  and  $w_{Kxy}$  and, in particular, for low to medium wind shear (i.e.,  $K < 0.005\text{ s}^{-1}$ ) the latter two are negligible with respect to  $w_S$  for any choice of antenna beamwidth  $\theta_{3dB}$ .
- 2) Assuming that the wind shear is equally shared among the orthogonal components, the contribution of  $w_{Kh}$  is negligible with respect to  $w_{Kxz}$  and  $w_{Kxy}$  for small  $\theta_{3dB}$ . Furthermore,  $w_{Kh}$  is always negligible with respect to  $w_S$ .
- 3) Spaceborne atmospheric radars are typically required to have a range resolution of 500 m or less. Therefore the contribution of  $w_{Kxz}$  is not negligible with respect to  $w_{Kxz}$  and  $w_{Kxy}$  only for very small antenna footprints (i.e., for  $\theta_{3dB} h_s$  comparable to  $0.35 c \tau_{pulse} a^{0.5} \cong 500\text{m}$ ).

In general, we have that contribution of wind shear can be neglected, and the Doppler width is determined mainly by the term  $w_S$  for  $\theta_{3dB}^2 \gg (w_T 2 a^{0.5} / v_s)^2$ . That is, for  $\theta_{3dB} > 0.15^\circ$  one has that  $w \cong w_S$  independently of the amount of turbulence and spread of terminal velocities. For smaller beamwidths, instead, the contribution of the terms depending on the characteristics of the rainfall field cannot be neglected, and, in general, a non constant  $w$  results from NDPR observations.

A measure of the correlation of two consecutive pulses under the assumption of Gaussian Doppler spectrum is given by the normalized spectral width  $w_N = w / 2v_m$ . By noting that  $\theta_{3dB} \cong \gamma \lambda / L_a$ , where  $L_a$  is the antenna diameter and  $\gamma$  is typically  $\sim 1.25$ , it follows that the contributions of  $w_s$  and  $w_K$  to the normalized spectral width  $w_N$  do not depend significantly on the choice of radar wavelength  $\lambda$  but only on the antenna size. On the other hand the contribution of  $w_D$  and  $w_T$  (which do not depend on  $\theta_{3dB}$ ), tend to broaden the spectrum when smaller  $\lambda$  are used.

In general, broader normalized spectra, correspond to weaker correlation between two consecutive pulses. The range of  $w_N$  that can be achieved with NDPR is determined mainly by the limitations on the maximum antenna size and by the range-ambiguity constraints imposed on the PRF.

However, the PRF upper bound is determined by the thickness of the atmosphere layer to be monitored. For precipitation measurements at a scanning angle  $\beta$  we have:

$$\frac{1}{PRF} = T_s > \frac{2H}{c} \frac{1}{\cos(\beta)} \quad (12)$$

where  $H$  is the extent of range interval with non-zero backscatter [in general it is assumed to be 20 km or less for spaceborne radar measuring precipitation, accounting also for the presence of the mirror image return]. Therefore, PRF up to 8000Hz could be assumed for scanning strategies with small  $\beta$ . However lower PRF must often be adopted because of the practical problems arising from the long and non-constant slant range of a spaceborne down-looking radar and/or from the choice of using long radar pulses to apply pulse-compression techniques.

Indeed, condition (6) poses a serious obstacle for obtaining low  $w_N$ . In fact, while an antenna of 10m could provide spectra with  $w_N$  similar to that of airborne radars [i.e.,  $w_N < 0.1$ ], obvious economical and technological requirements lead to the choice of smaller antennas, whenever possible. On the other hand, a 2 m antenna such as that of the TRMM Precipitation Radar (PR) or the one planned for the dual frequency precipitation radar of the GPM mission, even if PRF = 8000 kHz is considered, would generate spectra with  $w_N > 0.3$ , unsuitable for accurate estimates of any spectral moment of precipitation (other than the zero-order moment, that is, the power). Therefore, antenna diameters between 3 and 6 meters are considered as the region where to look for the optimal trade-off, for the purpose of radar system and

mission design. The corresponding range of  $w_N$  is between 0.1 and 0.3. Table 1 summarizes the  $w_N$  resulting from different choices of operating wavelength, PRF and antenna size, as well as three different turbulence regimes.

The feasibility of measurements of mean Doppler velocity from Gaussian spectra is generally checked through the condition<sup>2</sup>  $w_N < 1/2\pi$ . However, as discussed later, such threshold is relevant mainly to a specific group of spectral moments estimators(SME), the Pulse Pair processing, while it is not as significant when Fourier Analysis is adopted. For this reason, also system configurations leading to  $w_N > 1/2\pi$  are considered in this study and their performance in measuring the mean Doppler velocity are assessed. Uniform sampling is considered throughout the paper: while the use of polarization or frequency diversity methods would increase the available number of samples, and approaches like staggered PRF would extend the unambiguous ranges (i.e., relieving from the limitation imposed by Eq. 6), they do require additional technological considerations for a spaceborne application and are not addressed here.

### 2.1 Non Uniform Beam Filling conditions (NUBF)

It has been shown that spacecraft motion is the most relevant contribution to the spectral broadening for a wide range of system configurations. Indeed, such broadening can reduce the performance of spectral moment estimators, but it does not alter the fact that the first order moment of the spectrum corresponds to the mean Doppler velocity of the target.

On the other hand, when the rainfall field is not homogeneous, the spectral contributions from different portions of the radar volume of resolution are weighed unevenly. In terms of (2), one has that  $\eta_R(\mathbf{p}, v)$  does depend on  $\mathbf{p}$ . Therefore, the power spectrum is not given by the convolution of two approximately Gaussian functions [i.e.,  $\eta_R(\mathbf{p}, v)$  and  $W(\mathbf{p})$ ] as it was in the case of a homogeneous rainfield within the radar volume of resolution. Instead, a relation between the shape of the Doppler spectrum and the along-track profile of radar reflectivity for each range cell was found<sup>1</sup>.

It follows that, in NUBF conditions, the first moment of the Doppler spectrum does not correspond to the rainfall mean Doppler velocity. Instead, it includes an offset determined by the along-track position of the ‘center of mass’ of the along-track reflectivity profile  $Z_N(x)$  weighed by the antenna pattern. Such offset adversely affects mean Doppler velocity estimates, and it cannot be overcome through the standard SME algorithms. A Combined Time-Frequency (CFT) signal processing technique has been proposed to overcome the NUBF-induced offset<sup>6</sup>. The technique relies on the availability of Doppler spectra measured on volumes of resolution partially overlapped in the along-track direction in order to reconstruct the ‘history’ of the Doppler signature of each group of scatterers with equal relative velocity as the antenna footprint moves across them in the along-track direction. It was shown that the shape of such history (hereinafter referred to as a spectral track) is determined mainly by the shape of the antenna mainlobe pattern, which

TABLE I. NORMALIZED SPECTRUM WIDTH

$w_T$	Ku band (13.6 GHz)							Ka band (35 GHz)							W band (94 GHz)						
	$L_a$	2	3	4	5	6	10	$L_a$	2	3	4	5	6	10	$L_a$	2	3	4	5	6	10
	$\theta_{s,alt}$ PRF	.76	.51	.38	.30	.25	.15	$\theta_{s,alt}$ PRF	.29	.20	.15	.12	.10	.06	$\theta_{s,alt}$ PRF	.11	.07	.05	.04	.04	.02
1	5	.50	.34	.25	.20	.17	.10	5	.51	.34	.26	.21	.17	.11	5	.52	.36	.28	.24	.21	.16
	6	.42	.28	.21	.17	.14	.09	6	.42	.28	.21	.17	.15	.09	6	.43	.30	.23	.20	.17	.13
	7	.36	.24	.18	.14	.12	.07	7	.36	.24	.18	.15	.12	.08	7	.37	.26	.20	.17	.15	.11
	8	.32	.21	.16	.13	.11	.06	8	.32	.21	.16	.13	.11	.07	8	.32	.22	.18	.15	.13	.10
3	5	.51	.34	.26	.21	.18	.11	5	.52	.36	.29	.25	.22	.17	5	.63	.50	.45	.43	.41	.39
	6	.42	.28	.22	.17	.15	.10	6	.44	.30	.24	.20	.18	.14	6	.52	.42	.38	.36	.34	.32
	7	.36	.24	.18	.15	.13	.08	7	.37	.26	.21	.18	.16	.12	7	.45	.36	.32	.30	.29	.28
	8	.32	.21	.16	.13	.11	.07	8	.33	.23	.18	.15	.14	.11	8	.39	.32	.28	.27	.26	.24
5	5	.51	.35	.27	.22	.19	.14	5	.56	.41	.34	.31	.29	.25	5	.80	.71	.68	.66	.65	.63
	6	.43	.29	.22	.18	.16	.11	6	.46	.34	.29	.26	.24	.21	6	.67	.59	.56	.55	.54	.53
	7	.37	.25	.19	.16	.14	.10	7	.40	.29	.25	.22	.21	.18	7	.57	.51	.48	.47	.46	.45
	8	.32	.22	.17	.14	.12	.08	8	.35	.26	.21	.19	.18	.16	8	.50	.44	.42	.41	.41	.40

can be generally approximated by a Gaussian. Therefore, the results obtained for homogeneous conditions can be extended to the NUBF case by accounting for the different observation mode and signal processing approach as follows: the spectral track within the unambiguous Doppler range  $-v_m$  to  $+v_m$  requires  $T_T$  seconds to complete, where:

$$T_T = \frac{PRF \cdot \lambda \cdot h_s}{2 \cdot v_s^2} \quad (13)$$

during such time one can acquire up to  $N = T_T/(M/PRF)$  spectra of  $M$  points each. In CFT each spectral track is extracted from the time sequence of spectra with a resolution equal to the lower between the Doppler resolution and the time resolution (i.e., the number of points per spectral track is  $M_T = \min\{M, N\}$ ) and the time-spacing between two consecutive spectral tracks is  $T_{T0} = (M_T/PRF)$ . Once the desired minimum detectable size  $\Delta x$  of raincell is defined,  $N_T = \Delta x/(T_{T0} v_s)$  spectral tracks are averaged in time to improve accuracy. It follows that in first approximation, CFT performances are not sensitive to the choice of  $M$  as long as all spectra are available (i.e., if a constant pointing direction is used for the radar beam). The resulting equivalent number of samples  $M_{CFT}$  is given by:

$$M_{CFT} = \frac{\Delta x PRF}{v_s} \quad (14)$$

When cross-track scanning is considered as a valuable option for the observational strategy one should account for the 'loss' of the beams by assuming  $M'_{CFT} = M_{CFT}/N_C$  where  $N_C$  is the number of cross track beams per scan. However, this should be only the first step in the assessment of performance change: in fact, CFT performances will degrade rapidly as soon as the same-beam revisit interval rises past either a half radar footprint or the horizontal size of the observed raincell. Also, CFT performances will degrade for a choice of small  $M$  following the increase of DFT-related artifacts due to the finite spectral resolution and aliasing.

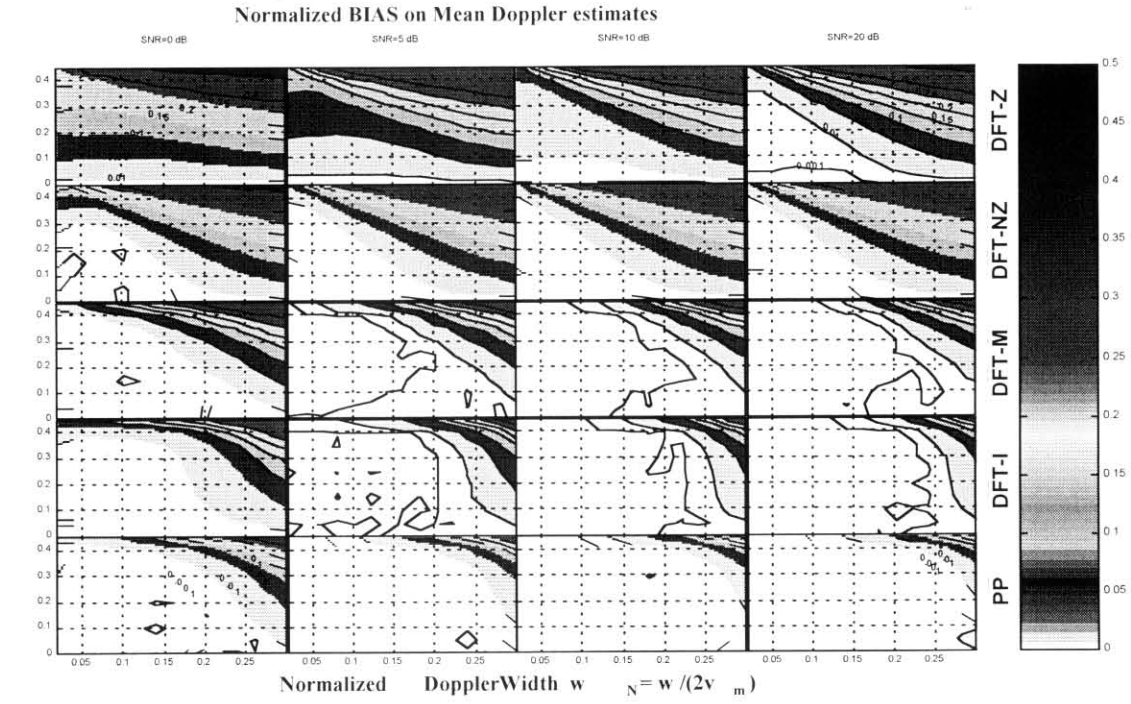
### 3. ESTIMATION OF MEAN DOPPLER VELOCITY

In this section the performance of three groups of SME. Pulse Pair processing (PP), Spectral Analysis (DFT) and CFT are analyzed with regards to their use on NDPR. In general, four parameters must be accounted for when assessing the performances of a SME in providing mean Doppler velocity estimates  $\hat{v}$  of a Gaussian Doppler spectrum:

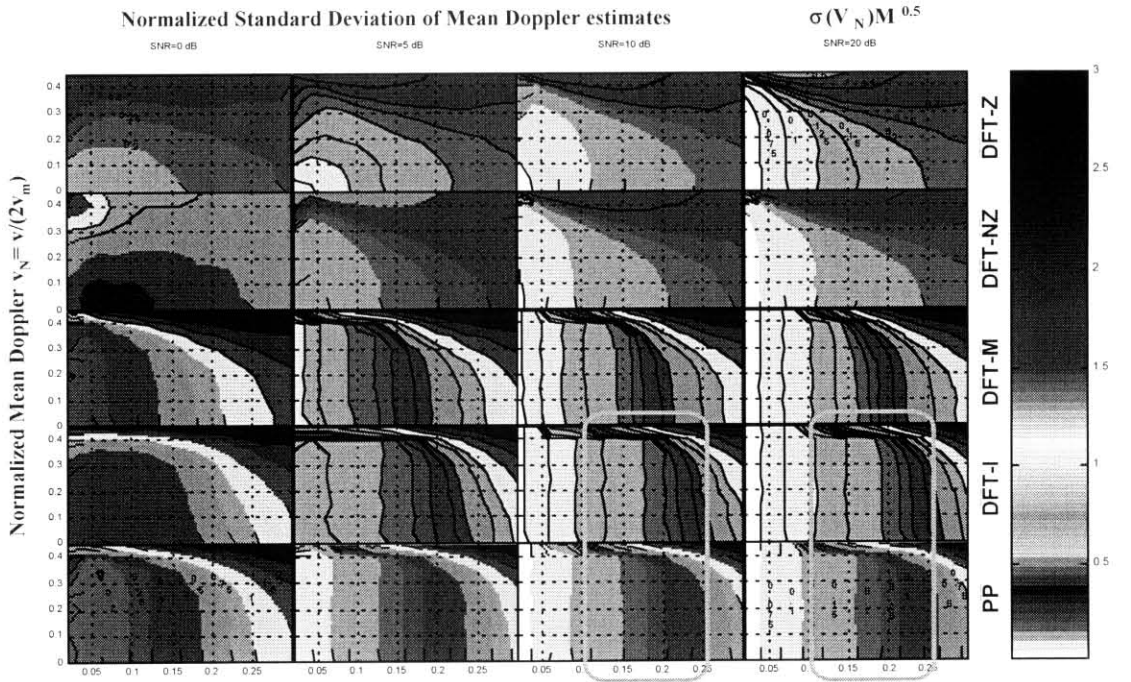
- 1) the normalized spectrum width  $w_N$  has been discussed in previous Section. As long as no significant portion of the Doppler spectrum is aliased [i.e., falls outside of the Nyquist limit  $v_m$ ] larger  $w_N$  yield larger a variance on mean Doppler estimates but do not introduce a bias.
- 2) the (true) normalized mean Doppler velocity  $v_N$  plays an important role when it causes a significant portion of the spectrum to fall beyond the Nyquist limit  $v_m$ , [e.g., when  $v_m - |v_N| < w_N/2$ ]. In this case, not only larger variances are expected but also a bias (towards zero Doppler) is introduced in  $\hat{v}$ .
- 3) The Signal to Noise Ratio (SNR). In general, white noise reduces pulse correlation hence increasing  $\text{var}(\hat{v})$  and biasing the estimates towards zero Doppler.
- 4) The number of pulses  $M$ . In general,  $\text{var}(\hat{v}) \propto M^{0.5}$ . Therefore large  $M$  are often sought to increase Doppler estimation accuracy. On the other hand, bias( $\hat{v}$ ) is not affected by the choice of  $M$ .

#### 3.1 Standard Spectral Moments Estimators

The PP estimator calculates the first two moments of the Doppler spectrum from estimates of the autocovariance function at time lag  $T_s$ . It is the most computationally efficient estimator available, and it performs almost optimally for narrow, symmetric spectra. For this reasons it is the most widely used estimator in ground-based and airborne weather radars, and it has been applied to several configurations including contiguous vs. independent pairs, alternate-polarization pairs, etc. The use of this estimator in NDPR, however, is adversely affected by its sensitivity to spectral width [i.e., exponential dependence on  $w_N$ ].



a)



b)

Figure 1. Normalized Bias and Normalized Standard Deviation of estimates of mean Doppler velocity estimates as function of SNR, normalized spectral width, normalized mean Doppler velocity and choice of SME.

The DFT estimator calculates the spectral moments directly from an estimate of the Doppler spectrum (here referred to as periodogram). The availability of hardware implementations of the Fast Fourier Transform make it extremely attractive for a spaceborne Doppler Precipitation radar. In fact, DFT performs better than PP in the 0.15-0.25 range of  $w_N$ . Furthermore, it allows more in depth analysis of the characteristics of the Doppler spectrum. This feature is extremely useful when the spectrum is not Gaussian (for example in NUBF conditions spectral processing is required in order to implement the CFT).

The defining equation of a generic DFT estimator is:

$$\hat{v}^{DFT} = -\frac{\lambda}{2MT_S} \left\{ \hat{m}' + \frac{1}{(S_p + S_N) - \hat{S}_N} \sum_{m=\hat{m}'-M/2}^{\hat{m}'+M/2} (m - \hat{m}') \cdot \left[ (P_{\text{mod}_M(m)} + N_{\text{mod}_M(m)}) - \hat{N}_{\text{mod}_M(m)} \right] \right\} \quad (15)$$

where  $S_p$  and  $S_N$  are the signal and noise power, respectively, the hat indicates an estimate,  $P_m$  is  $m$ -th line of the power spectrum as calculated through DFT of  $M$  complex voltage samples (periodogram), and  $m_0'$  is the number of a specific frequency bin in which the initial estimate  $a$  of the mean spectral frequency is made (i.e.,  $m_0' = aM/PRF$ ).

The four algorithms are different in their ways of handling of noise and strategy for obtaining the initial guess  $a$ . The first algorithm, referred to as DFT-Z, assumes  $m_0' = 0$ . It does not remove any white noise contribution (i.e.,  $= 0$  in (15)), which makes it a biased estimator at low SNR's. The second algorithm, referred to as DFT-ZN, also assumes  $m_0' = 0$  but it removes the nominal (estimated) noise power in order to eliminate the bias due to white noise. However, at low SNR's the standard deviation of (15) for DFT-ZN is significantly higher than that for DFT-Z<sup>7</sup>.

The third algorithm, referred to as DFT-M, was suggested in 2. It assumes  $m_0'$  to be equal to the number of the frequency bin which has the largest power (i.e.,  $=$ ), and it does not remove any white noise contribution. For narrow spectra (e.g.,  $w_N < 0.1$ ) and large  $M$  (e.g.,  $M > 1000$ ), this algorithm provides unbiased estimates of the first spectral moment with the corresponding standard deviations comparable to those obtained by DFT-Z. However, this algorithm is more sensitive to  $w_N$  than DFT-Z and DFT-ZN<sup>8</sup>.

The fourth algorithm, referred to as 'two-step' DFT algorithm (DFT-2), was introduced<sup>1</sup> to provide better performances for spaceborne applications. In the first step of this algorithm, (15) is applied with  $m_0' = 0$  and the noise is set to the nominal value to obtain a first velocity estimate. The noise density estimate is then updated by setting it equal to the minimum of the smoothed periodogram. In the second step, a refined velocity estimate is obtained through (15) with  $a$  equal to the previous estimate and with the updated noise estimate. This second step can be repeated until the change in mean Doppler estimate falls below a specified threshold. In general, this algorithm is capable of providing unbiased estimates with standard deviations comparable to DFT-Z. For mean vertical velocities close to the Nyquist limit, it shows a multimodal distribution of the mean velocity estimate, with the secondary modes appearing at the aliased images ( $\pm 2v_m$ ) of the true mean Doppler velocity and at the mid-position corresponding to a low portion of the spectrum ( $\pm v_m$ ). However, these secondary modes are easily removed by checking if the estimate belongs to the Nyquist range or if it is in a region of low spectral density.

Perturbation analysis was used to derive  $\text{var}(\hat{v})$  for PP and DFT estimators under the hypothesis of narrow spectrum<sup>7</sup>. That approach has been extended<sup>8</sup> for NDPR to apply to spectra with  $w_N < 0.3$ . The analytical results were in excellent agreement with the results of Monte Carlo simulations performed on periodograms simulated as described in 9. Figure 1 shows the results of the simulations for the PP algorithm for contiguous pairs and for 4 versions of the DFT estimator.

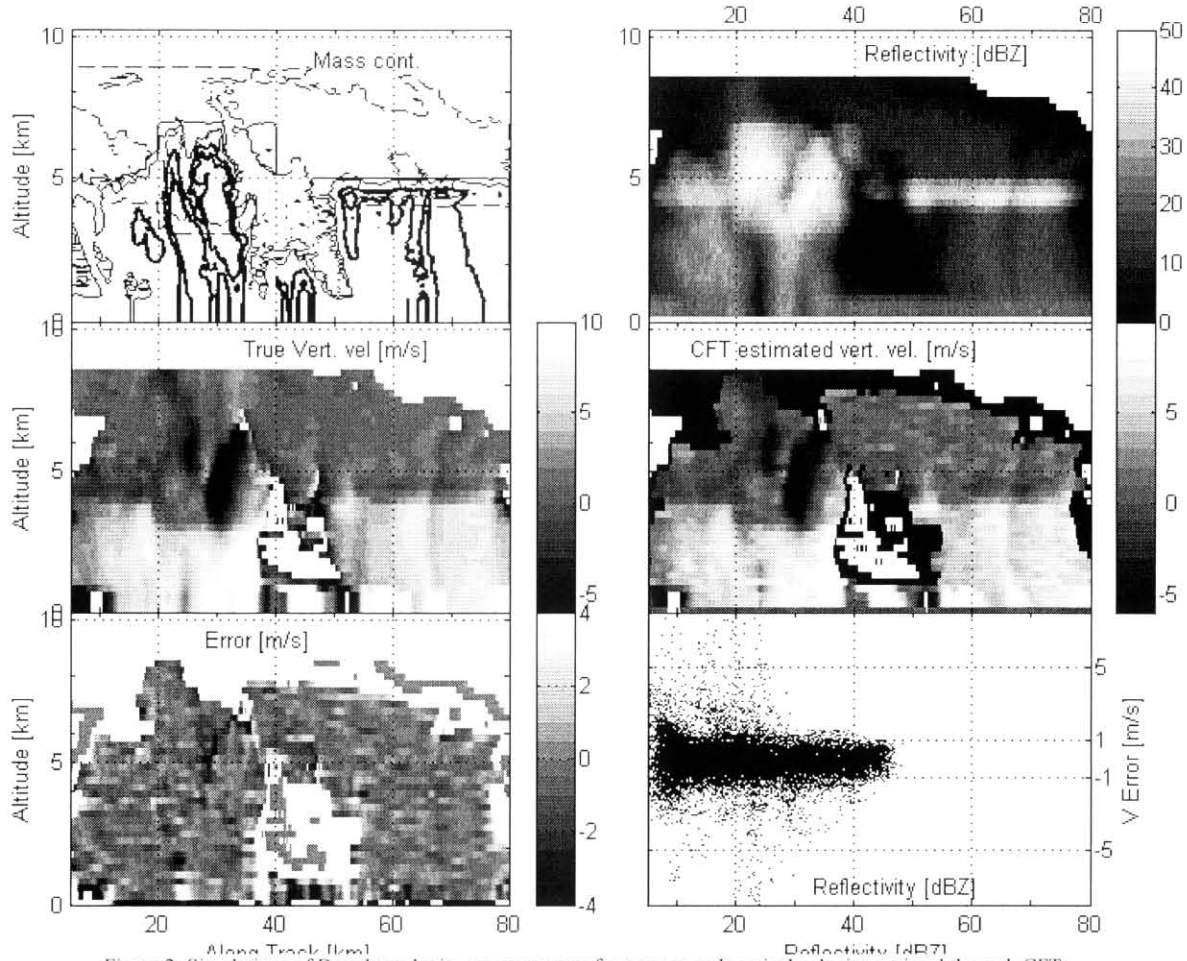


Figure 2. Simulations of Doppler velocity measurements from space and vertical velocity retrieval through CFT.

## CONCLUSIONS

The results shown in this paper provide a first assessment of the performances expected by a specific configuration of Doppler Precipitation Radar. As an example we can determine the performances for a Nadir Pointing Ku-band radar on a LEO platform, with  $L_a = 5$  m,  $PRF=6$  KHz and using CFT to compensate for NUBF effects: from Table 1 we obtain  $w_N = 0.17$  for a moderate turbulence regime. Since DFT-I is used in CFT, Figure 1 shows that for  $SNR > 10$  dB no significant bias in the estimator is expected in the range  $\pm 26.5$  m/s and the predicted standard deviation is  $\sim 13.5/M_{CFT}$  m/s. Requiring a minimum raincell size of  $\Delta x = 0.5$  km, one obtains a final estimate of the standard deviation (after CFT processing) in mean Doppler velocity estimates of  $\sim 0.65$  m/s. Results of simulations<sup>6</sup> performed through a 3D spaceborne Doppler radar simulator applied to high resolution datasets (such as that shown in Figure 2 for the discussed configuration) generally confirm this method of assessing performances. However, one should always account for the approximations adopted to obtain such a general method and carefully verify that all intermediate hypothesis are met. Overall, several configurations of the radar system are capable of providing mean Doppler velocity measurements with an accuracy of 1 m/s or better.

## ACKNOWLEDGEMENT

The research described in this paper was performed at the Jet Propulsion Laboratory, California Institute of Technology, under contract with the National Aeronautics and Space administration.

## REFERENCES

- [1] S. Tanelli, E. Im, S. L. Durden, L. Facheris and D. Giuli, "The effects of nonuniform beam filling on vertical rainfall velocity measurements with a spaceborne Doppler radar", *J. Atmos. Oceanic Technol.*, vol-19, 2002, pp. 1019-1034. R. J. Doviak and D. S. Zrnic, *Doppler radar and weather observations*, Academic Press, 1993.
- [2] D. S. Zrnic, "Estimation of spectral moments for weather echoes", *IEEE Trans. on Geosc. Electr.*, vol-4, pp. 113-128, 1979.
- [3] D. Sirmans and B. Bungarner, "Numerical comparison of five mean frequency estimators", *J. Appl. Meteor.*, vol-14, pp. 991-1003, 1975.
- [4] R. Meneghini and T. Kozi, *Spaceborne Weather Radar*, Artech House Ed., 1990.
- [5] S. Kobayashi, "A Unified formalism of incoherent, quasi-coherent, and coherent correlation signals on Pulse-Pair Doppler operation for a cloud-profiling radar: aiming for a space mission". *J. Atm. Oce. Tech.*, vol-19, 2002, pp.443-456.
- [6] S. Tanelli, E. Im, S.L. Durden, L. Facheris. D. Giuli and E.A. Smith, "Rainfall Doppler Velocity Measurements from Spaceborne Radar: Overcoming Nonuniform Beam-Filling Effects", *J. Atm. Oce. Tech.*, **21**, 2004, pp.27-44.
- [7] Sirmans D. and B. Bungarner, 1975: Numerical comparison of five mean frequency estimators. *J. Appl. Meteor.*, 14, 991-1003.
- [8] Tanelli S., E. Im, L. Facheris and E. A. Smith, 2002 DFT-based spectral moment estimators for spaceborne Doppler precipitation radar, to appear on Proc. of Third International Asia-Pacific Symposium on Remote Sensing of the Atmosphere, Environment and Space (SPIE Vol. 4894), Hangzhou (RPC), Oct. 23-27 2002.
- [9] Zrnic D.S. 1978: Simulation of weatherlike Doppler Spectra and Signals, *J. App. Meteor.*, 14, pp. 619-620